15423

Offer #06MV-26

Robust Control Techniques for State Tracking in the Presence of Variable Time Delays

Jarrett Goodell, Marc Compere, Miguel Simon, Wilford Smith, Ronnie Wright
Science Applications International Corporation

Mark Brudnak
U.S. Army TARDEC

ABSTRACT

In this paper, a distributed driver-in-the-loop and hardware-in-the-loop simulator is described with a driver on a motion simulator at the U.S. Army TARDEC Ground Vehicle Simulation Laboratory (GVSL). Realistic power system response is achieved by linking the driver in the GVSL with a full-sized hybrid electric power system located 2,450 miles away at the TARDEC Power and Energy Systems Integration Laboratory (P&E SIL), which is developed and maintained by Science Applications International Corporation (SAIC). The goal is to close the loop between the GVSL and P&E SIL over the Internet to provide a realistic driving experience in addition to realistic power system results. In order to preserve a valid and safe hardware-in-the-loop experiment, the states of the GVSL must track the states of the P&E SIL. In a distributed control system utilizing the open Internet, the communications channel is a primary source of uncertainty and delay that can degrade the overall system performance and stability. The presence of a cross-country network delay and the unavoidable differences between the P&E SIL hardware and GVSL model will cause the GVSL states and P&E SIL states to diverge without any additional action. Thus, two robust strategies for *state convergence* are developed and presented in this paper. The first strategy is a non-linear Sliding Mode control scheme. The second strategy is an H-infinity control scheme. Both schemes are implemented in simulation, and both schemes show promising results for *state convergence* in the presence of variable cross-country time delays.

INTRODUCTION

TARDEC is developing a comprehensive Power Budget Model (PBM) to project the power and energy usage of each entity on the battlefield. This will provide the user community with a tool to assist in making informed decisions concerning force structure and vehicle designs. The PBM provides a power estimation and control capability at both the vehicle level and at the unit level that aggregates multiple vehicles and multiple players. At the vehicle level, it provides the capability to calculate automotive performance along with the capabilities of the power supply to provide timely and sufficient energy to each load, both on- and off-vehicle. The PBM is a four-phase effort, progressing from Phase 0 to Phase 3. Phase 0 is the existing desktop CHPSPerf tool that can be used to approximate the power from a single vehicle. Phase 3, otherwise known as the *RemoteLink*, is a coupled hardware-in-the-loop / driver-in-the-loop networked multi-vehicle simulation of the future battlefield. This PBM tool version will couple existing TARDEC laboratory facilities, namely a six-degree-of-freedom motion base/crew station in Warren, MI and the P&E SIL power system located in San Jose, CA. The motion base will provide driving realism while the P&E SIL will provide a realistic hardware power system response

The goal of the *RemoteLink* is to provide a real-time cross-country link that causes the GVSL's motion-base and P&E SIL's power system hardware to interact together as if they were both connected locally. Both the GVSL and P&E SIL will contain coupled dynamic systems that create a seamless simulation environment for realistically exercising the power train hardware located in San Jose, CA. Remote operation of the P&E SIL hardware is initiated by a human operator in a driving simulation environment located in Warren, MI where a vehicle dynamics model is simulated locally to drive a motion base simulator. These two test sites are separated by 2,450 miles (see Figure 1) but communicate over the open Internet. Use of the open Internet as a communication channel to couple these two dynamic systems poses several problems [1] including significant time delay, variable time delay, and data loss.

Four strategies have been identified as keys to implementation of the *RemoteLink*.

1. Local power system model: A dynamic model of the entire SIL power system, CHPSPerf [2,4], will run on the crewstation motionbase. This model will provide an estimate of the real power system

Report Documentation Page

Form Approved
OMB No. 0704-0188

1. REPORT DATE	2. REPORT TYPE	3. DATES COVERED
10 JAN 2005	**Journal Article**	**10-01-2005 to 10-01-2005**

4. TITLE AND SUBTITLE	5a. CONTRACT NUMBER
ROBUST CONTROL TECHNIQUES FOR STATE TRACKING IN THE PRESENCE OF VARIABLE TIME DELAYS	**DAA-E07-02-C-L045**
	5b. GRANT NUMBER
	5c. PROGRAM ELEMENT NUMBER
6. AUTHOR(S)	5d. PROJECT NUMBER
Jarrett Goodell; Marc Compere; Miguel Simon; Mark Brudnak	5e. TASK NUMBER
	5f. WORK UNIT NUMBER
7. PERFORMING ORGANIZATION NAME(S) AND ADDRESS(ES)	8. PERFORMING ORGANIZATION REPORT NUMBER
Science Applications International Corporation,8303 N. Mopac Expwy, Suite B-450,Austin,TX,78759	**; #15423**
9. SPONSORING/MONITORING AGENCY NAME(S) AND ADDRESS(ES)	10. SPONSOR/MONITOR'S ACRONYM(S)
U.S. Army TARDEC, 6501 E.11 Mile Rd, Warren, MI, 48397-5000	**TARDEC**
	11. SPONSOR/MONITOR'S REPORT NUMBER(S)
	#15423

12. DISTRIBUTION/AVAILABILITY STATEMENT

Approved for public release; distribution unlimited

13. SUPPLEMENTARY NOTES

SAE WORLD CONGRESS 2006 COBO HALL, DETROIT, MI

14. ABSTRACT

In this paper, a distributed driver-in-the-Ioop and hardware-in-the-Ioop simulator is described with a driver on a motion simulator at the U.S. Army TARDEC Ground Vehicle Simulation Laboratory (GVSL). Realistic power system response is achieved by linking the driver in the GVSL with a full-sized hybrid electric power system located 2,450 miles away at the TARDEC Power and Energy Systems Integration Laboratory (P&E SIL), which is developed and maintained by Science Applications International Corporation (SAIC). The goal is to close the loop between the GVSL and P&E SIL over the Internet to provide a realistic driving experience in addition to realistic power system results. In order to preserve a valid and safe hardware-in-the-Ioop experiment, the states of the GVSL must track the states of the P&E SIL. In a distributed control system utilizing the open Internet, the communications channel is a primary source of uncertainty and delay that can degrade the overall system performance and stability. The presence of a cross-country network delay and the unavoidable differences between the P&E SIL hardware and GVSL model will cause the GVSL states and P&E SIL states to diverge without any additional action. Thus, two robust strategies for state convergence are developed and presented in this paper. The first strategy is a non-linear Sliding Mode control scheme. The second strategy is an H-infinity control scheme. Both schemes are implemented in simulation, and both schemes show promising results for state convergence in the presence of variable cross-country time delays.

15. SUBJECT TERMS

16. SECURITY CLASSIFICATION OF:			17. LIMITATION OF ABSTRACT	18. NUMBER OF PAGES	19a. NAME OF RESPONSIBLE PERSON
a. REPORT **unclassified**	b. ABSTRACT **unclassified**	c. THIS PAGE **unclassified**	**Same as Report (SAR)**	**9**	

Standard Form 298 (Rev. 8-98)
Prescribed by ANSI Std Z39-18

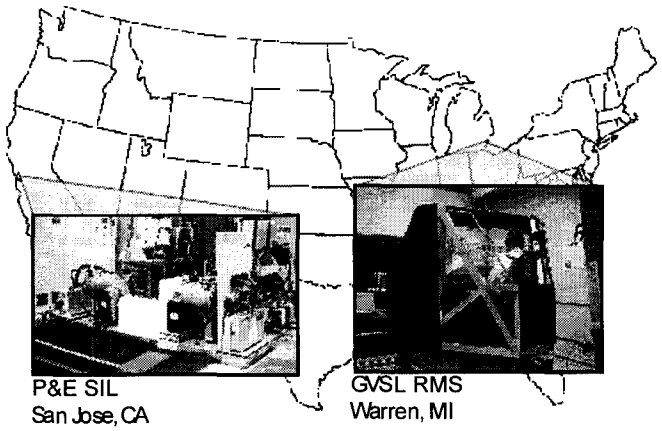

Figure 1. Illustration of long haul components.

hardware's response to the motion base vehicle model.

2. Adaptive filtering algorithm: A Kalman or RLS filter will provide real-time updates to the GVSL mobility model's torque inputs [3].

3. State convergence: A method for observing and coordinating pertinent dynamic states for both the mobility and power system models is implemented at both ends. This paper discusses *state convergence* in detail.

4. Parameter tuning: Future work includes both offline and online parameter estimation for the power system model. CHPSPerf is validated against experimental data, however, both extended hardware operation and temperature-dependent effects present a need for continued power system parameter estimation.

The use of CHPSPerf and the adaptive filtering strategy have shown potential to minimize the unwanted effects of time delay, but also introduce the need for coordination between the states of the GVSL and the P&E SIL. Although both delay compensation and coordination of the GVSL and P&E SIL states are addressed in the *RemoteLink*, this paper discusses the solution to the latter of these problems, which is called *state convergence* throughout the remainder of the paper. The *state convergence* algorithms are observers which cause the states in the GVSL power system model to track the states of the real power system hardware. This observer is called the *powertrain observer*. Similarly, the states in the P&E SIL vehicle model should track the states of the GVSL vehicle model. This observer is called the *vehicle dynamics observer*. Two robust control strategies for achieving *state convergence* are presented, including a non-linear Sliding Mode control scheme and an H-infinity control scheme. This paper covers the following discussions: the *RemoteLink* high-level problem formulation and system description, design strategies and implementations, experimental results, followed by a conclusion and future work.

SYSTEM DESCRIPTION AND PROBLEM FORMULATION

Figure 2 illustrates the interfaces between the GVSL and P&E SIL, which are separated by a distance of 2,450 miles. The GVSL (shown in the top half of Figure 2) consists of three main features. The first is the driver, who operates a crewstation mounted on a motion simulator. The crewstation receives both visual and motion feedback which provides the driver with a realistic driving experience and the P&E SIL power system with realistic driver commands. In order to provide feedback to the driver, the crewstation and motion simulator both use vehicle states from the local vehicle model, which is the second important feature of the GVSL. This vehicle model is a high-fidelity, 3-D, real-time, multi-body

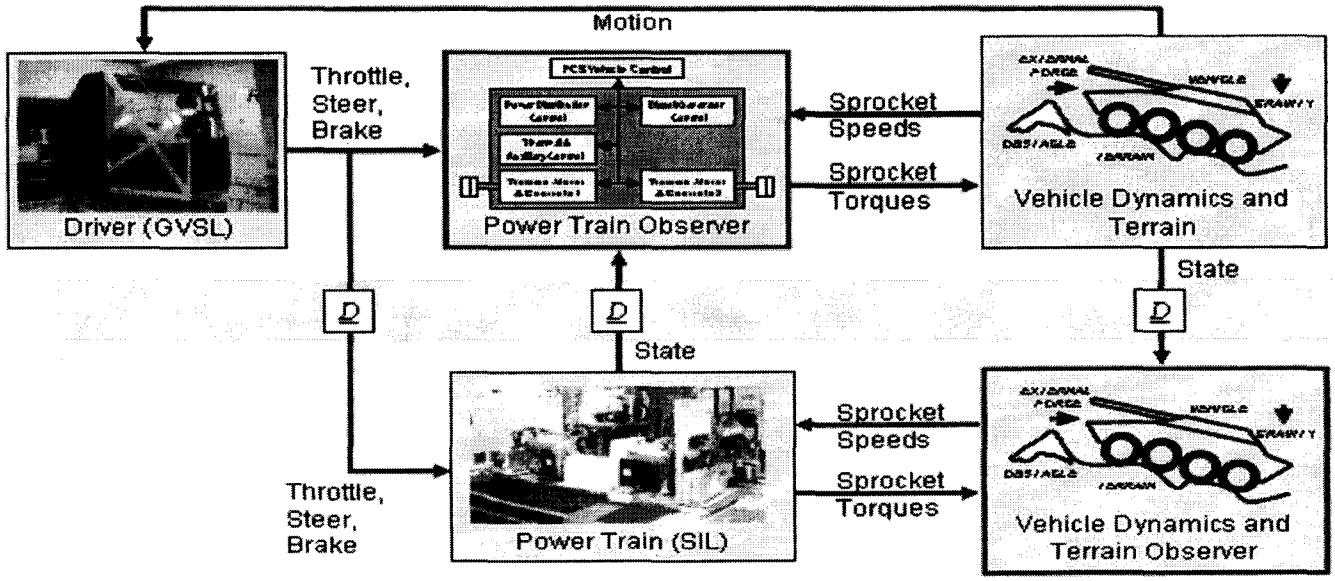

Figure 2: *RemoteLink* Architecture

dynamics model which receives sprocket torques from the power system model and sends vehicle states to the crewstation and motion simulator. The third GVSL feature is the CHPSPerf hybrid electric power system model [2]. The CHPSPerf power system is designed to closely model the hardware in the SIL and provides high frequency torque response to the GVSL vehicle model. These torques are computed based upon driver commands, vehicle states, local motor models, and torque data from the P&E SIL. The local CHPSPerf power system model must balance two objectives: 1) provide fast, realistic response to the driver to maintain realistic driver feel and 2) provide a response that closely resembles the behavior of the actual P&E SIL power system. In order to achieve these two objectives, a delay compensation strategy [3] was developed and resides in software inside the CHPSPerf power system model. Note that the power system torques are not physical torques, but are torques that exist in software.

With respect to the P&E SIL (shown in the bottom half of Figure 2), two major entities are present – the series hybrid power system hardware designed to power a 20-22 ton tracked vehicle and the vehicle model and dynamometers. The power system hardware receives a time delayed version of the driver inputs *(steering, throttle, and braking*) from the GVSL along with the vehicle speed from the SIL vehicle model and responds with actual traction motor torques. The vehicle model computes speed states and produces reaction torque commands which result from interaction with virtual terrain. These load torque commands are fed back to the power system through dynamometers that are connected to the traction motors. This load emulation process is described in more detail in [5]. On the SIL side, the *state convergence* algorithms reside in the vehicle model and should cause its states to track those of the vehicle model at the GVSL.

SYSTEM OPERATION

The system operation of the *RemoteLink* is initiated by driver inputs. Once the driver provides inputs (steering, throttle, braking) to the crewstation (shown in Figure 3), those inputs flow simultaneously to the GVSL and to the P&E SIL. However, the driver inputs must travel through the open Internet and across the country in order to reach the P&E SIL. Thus, the GVSL power system model receives driver inputs before the SIL power system hardware receives those same driver inputs. For reference purposes, suppose that the driver supplies commands at time t and that the one-way cross country Internet delay is a constant value of Δ. This implies that the driver won't feel the response from the SIL hardware until time $t+2\Delta$. If Δ is too large, the driver won't be able to navigate the vehicle in a stable fashion. This illustrates the importance of having the local power system model in the GVSL to give instantaneous response.

The downside to having a local power system model is that a model of a system can never perfectly match the physical system. Thus, the presence of the GVSL power system model introduces error between the GVSL torques and the P&E SIL torques. Therefore, it can be deduced that if the torques are in error, then other vehicle states such as sprocket speeds, velocity, and positions will be in error. Once the GVSL states become significantly different from the P&E SIL states, the driver-in-the-loop/hardware-in-the-loop experiment becomes meaningless and there are potential safety concerns for the motion base in the GVSL. Avoiding divergent states is the motivation for *state convergence* within the *RemoteLink*. The first method used to achieve *state convergence* is discussed in the next section.

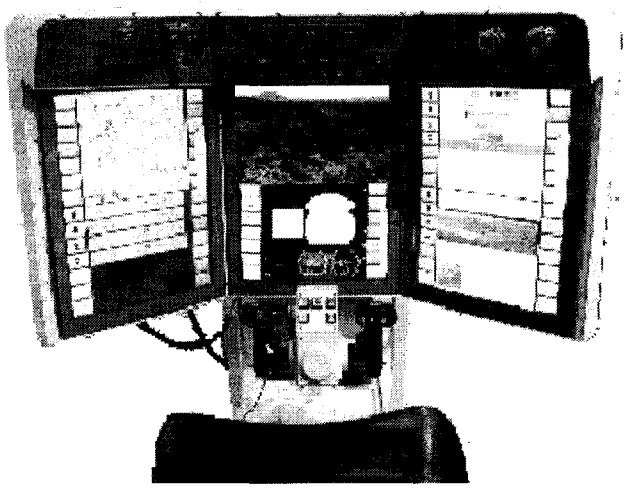

Figure 3: Crew station controls.

SLIDING MODE CONTROL APPROACH

A derivation of sliding mode control is outside the scope of this paper; however, the application of sliding mode control for *state convergence* is demonstrated. Before showing the application to this specific problem, first it is necessary to make a few general remarks about sliding mode control before going into detail about the control law for the *RemoteLink*. Sliding Mode control can transform a higher order tracking problem into a first-order stabilization problem [6]. The main idea of sliding mode control is to drive the states of the system to a desired area in state-space known as the sliding surface, which is defined by the designer. Let us assume that the system we are modeling has the form of

$$\begin{aligned} \dot{x} &= f(x) + b(x,t)u(t) \\ y &= h(x) \end{aligned} \tag{1}$$

where u is the control input, x is the state vector, and y the output vector.

In addition, suppose that the vector y represents the actual outputs, or states, of a system and the vector y_d represents the desired system outputs. A commonly used sliding surface [6] is shown in (2) below.

$$s(x,t) = (\frac{d}{dt} + \lambda)^{(n-1)} \tilde{y}(t) \quad (2)$$

where n is the relative order of the output, $\tilde{y}(t)$ is the output error $y(t) - y_d(t)$, and λ is a constant chosen by the designer.

In effect, this sliding surface, s, is an error surface. It is desirable to maintain this error surface at zero; hence, it is shown that this tracking problem is transformed into a first order stabilization problem in s. Not only is it desirable to maintain the error at zero, but it is also desirable to maintain the error rate-of-change at zero. Due to the fact that the order of (2) is (n-1), s only needs to be differentiated once for the input to appear. Taking the derivative of s and setting it equal to zero leads to a solution for the equivalent control term.

The equivalent term is an important and necessary component of sliding mode control, but an additional term is needed in order to maintain the sliding mode in the presence of disturbances, modeling simplifications and parametric uncertainties. This term is called the robust term. The robust term [6] typically takes the form $u_{rob} = -\eta \operatorname{sgn}(s)$, however the *state convergence* implementation is modified slightly to use the tanh() function,

$$u_{rob} = -\eta \tanh(s / s_0) \quad (3)$$

where η is a constant chosen by the designer and s_0 is a boundary layer width. Unlike the sgn() function the tanh() function is smooth near zero and with a properly sized boundary layer, eliminates chatter near $s = 0$.

Therefore, the robust term works by aggressively forcing the system back to the sliding mode when the states leave the boundary layer around the original sliding surface $s = 0$.

Now that a generalized methodology for deriving an effective sliding mode control has been provided, this methodology can be applied to the *RemoteLink*. In the case of the *RemoteLink*, the goal is to make the states of the P&E SIL vehicle model follow the states of the GVSL vehicle model. Two approaches can be taken with respect to *state convergence* of the vehicle states: 1) Force the P&E SIL states to track the GVSL states as quickly and abruptly as possible 2) Gradually migrate the P&E SIL states to track the GVSL states. In the interest of protecting the P&E SIL power system hardware, the second approach of gradually nudging the P&E SIL states is chosen.

The aforementioned states that must be converged include global X position, global Y position, velocity, left sprocket speed, right sprocket speed, and yaw angle. In the interest of being brief, the derivation is only shown for yaw angle *state convergence*. Derivations for the other states are similar to the following derivation for yaw angle *state convergence*.

The first step in deriving a sliding mode control law is obtaining the equivalent control term, and the first step in obtaining the equivalent control term is to write the equation of motion for the state of interest. Thus, (4) below shows the equation of motion for the vehicle yaw angle, Ψ.

$$\ddot{\psi} = \frac{\Sigma M_z - (\vec{\omega} \times \vec{J} \cdot \vec{\omega})_z}{J_{zz}} + p_\psi \quad (4)$$

where ψ is the yaw angle, M_z is the moment about the yaw axis, ω is the angular velocity of the vehicle, J is the vehicle rotational moment of inertia, and p_ψ is the *state convergence* control input.

As indicated in the above methodology for sliding mode control, the next step is to define a sliding surface for the control to follow. Accordingly, a sliding surface is defined in (5).

$$s = \dot{\tilde{\psi}} + \lambda \tilde{\psi} = \dot{\psi}_{sil} - \dot{\psi}_{gvsl} + \lambda(\psi_{sil} - \psi_{gvsl}) \quad (5)$$

Taking the time derivative of the sliding surface and setting the equation equal to zero reveals the following expression.

$$0 = \ddot{\psi}_{sil} - \ddot{\psi}_{gvsl} + \lambda(\dot{\psi}_{sil} - \dot{\psi}_{gvsl}) \quad (6)$$

Examining (6), we see that terms exist for the P&E SIL and for the GVSL. Note that the GVSL yaw rate and yaw acceleration terms are desired values coming across the network from the GVSL to the P&E SIL. In order to bring the control input term into this equation, the yaw acceleration defined in (4) must be substituted into (6). After re-arranging terms, (7) below shows the expression

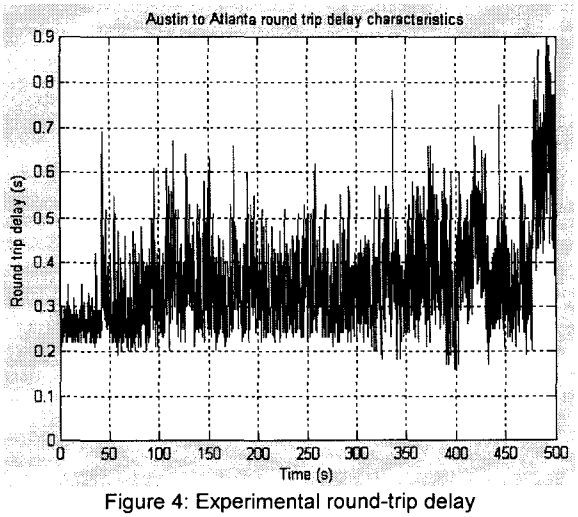

Figure 4: Experimental round-trip delay

for the equivalent control term.

$$p_{\psi,eq} = \ddot{\psi}_{gvsl} - \lambda(\dot{\psi}_{sil} - \dot{\psi}_{gvsl}) - \frac{\Sigma M_z - (\vec{\omega} \times \vec{J} \cdot \vec{\omega})_z}{J_{zz}} \quad (7)$$

As mentioned above, the GVSL terms are available information coming over the network connection. The P&E SIL terms are all accessible from the vehicle dynamics model in the P&E SIL. The equivalent control term is a necessary component of sliding mode control, but it alone is not enough to guarantee robust controller performance.

In order to withstand disturbances or modeling uncertainty, a second (robust) term is necessary, as defined in (3) above. The designer must choose the gain parameter η to be large enough such that the controller has enough authority to drive the states to within their boundary layers; however, if the gain parameter is chosen to be too large, this can cause numerical instability, chatter, and possibly excite unmodeled high-frequency system dynamics. The robust term is simply added with the equivalent term to get the complete non-linear sliding mode control in (8) below.

$$p_{\psi} = \ddot{\psi}_{gvsl} - \lambda(\dot{\psi}_{sil} - \dot{\psi}_{gvsl}) - \ldots \\ \ldots \frac{\Sigma M_z - (\vec{\omega} \times \vec{J} \cdot \vec{\omega})_z}{J_{zz}} - \eta \tanh(s / s_0) \quad (8)$$

The sliding mode control input shown in (8) is implemented into the tracked vehicle dynamics model [4] in the Matlab/Simulink simulation environment. Similar derivations are performed and implemented in simulation for the other five states that must be converged. Results for sliding mode control *state convergence* are shown in the next section.

RESULTS FOR SLIDING MODE CONTROL STATE CONVERGENCE

Testing for *state convergence* using sliding mode control was conducted by executing the GVSL simulation in Austin, TX and executing the P&E SIL simulation in Atlanta, GA. The two simulations transferred data back and forth by means of UDP connection. The simulation was run for a lap around the Churchville short course and lasted for a total of 500 seconds. The round-trip latencies experienced were variable and significant, as indicated in Figure 4.

In spite of the significant round-trip time delays, successful *state convergence* was demonstrated. Figure 5 below shows the position plot including both the GVSL and P&E SIL trajectories.

Similarly, the velocities for the GVSL and SIL tracked each other successfully. Figure 6 shows the velocity plot including both the GVSL and P&E SIL velocities.

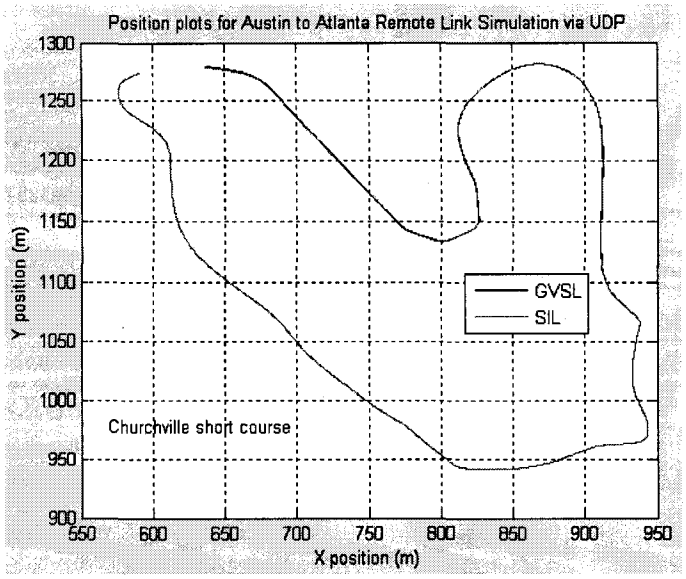

Figure 5: GVSL and P&E SIL Trajectories

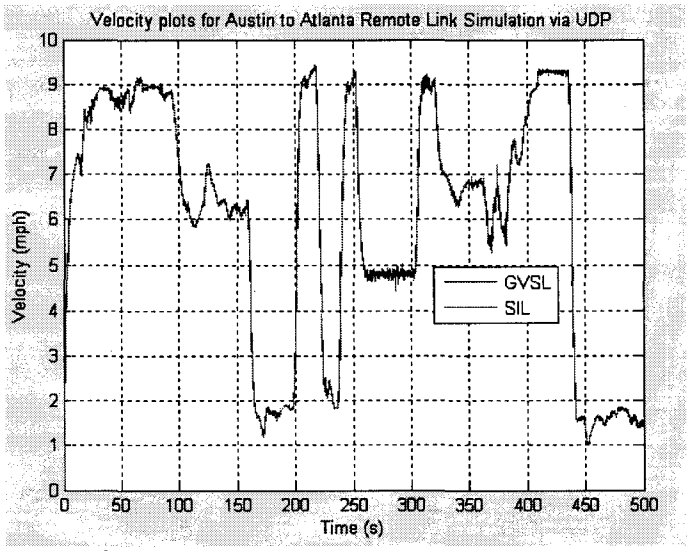

Figure 6: GVSL and P&E SIL Velocities

Even in the presence of significant and variable round-trip latencies, all six of the GVSL and P&E SIL states track successfully. In conclusion, the sliding mode control *state convergence* scheme derived in this study is successful and is ready for application in the P&E SIL as soon as the P&E SIL hardware is ready for remote operation.

H-INFINITY CONTROL APPROACH

This section discusses use of H-infinity for achieving *state convergence*. The remote link architecture in Figure 2 can be viewed as shown in Figure 7, where P is the nominal plant corresponding to the GVSL vehicle dynamics model, $\tilde{P}$ is the model plant corresponding to the SIL vehicle dynamics model, $\tilde{K}$ is the software based controller corresponding to the CHPSPerf power system model, and K is the hardware-in-the-loop controller in the P&E SIL corresponding to the SIL power system. Let Δ be a variable transport time delay with

unspecified phase as shown in Figure 7, then $\tilde{P}$ is a generalized plant modeled as a multiplicative perturbation on the nominal plant P given by

$$\tilde{P} = (1 + \Delta_P W_P) P \qquad \|\Delta_P\|_\infty \le 1 \qquad (9),$$

where $\|\Delta_P\|_\infty$ is the H-infinity norm of the arbitrary transport delay represented by the *variable* transfer function Δ_P and W_P is a fixed stable transfer function. The condition $\|\Delta_P\|_\infty \le 1$ allows a suitable performance weight $W_P(j\omega)$ to constraint the arbitrary time delay Δ_P. In equation (9), the term $\Delta_P W_P$ is a way to specify uncertainty, namely, the uncertainty model $\Delta_P W_P$ is a measure of how distant the normalized plant is from 1. That is, equation (9) tells us that when $\|\Delta_P\|_\infty \le 1$ then the nominal plant P and the generalized plant $\tilde{P}$ differ by the following factor.

$$\left| \frac{\tilde{P}(j\omega)}{P(j\omega)} - 1 \right| \le |W_P(j\omega)| \qquad \forall \omega \qquad (10)$$

Since P and $\tilde{P}$ differ by a pure time delay in Figure 4, then the following model applies. Let

$$\tilde{P}(s) = e^{-\tau s} P(s) \qquad (11)$$

where

$$\left| e^{-\tau j\omega} - 1 \right| \le |W_P(j\omega)| \qquad \forall \omega, \tau \qquad (12)$$

where the term $\left| e^{-\tau j\omega} - 1 \right|$ is a Pade approximation of a pure time delay given by:

$$\left| e^{-\tau s} - 1 \right| \approx \left| \frac{-\tau s + 1}{\tau s + 1} - 1 \right| = \frac{2\tau}{\tau s + 1} \qquad (13)$$

Equation (13) gives us a suitable expression for the performance weight W_P. For example, given a transport delay $\tau = 1/10$ seconds, then:

$$\frac{0.21s}{0.1s+1} \le W_P(s) = \frac{0.21s}{0.1s+1} \qquad \forall \omega, \tau = 0.1 \qquad (14)$$

Notice that the same technique of casting a transport delay into a multiplicative perturbation on a nominal plant is used for the controller as well. Consequently, a family of controllers can be obtained such that

$$\tilde{K} = (1 + \Delta_K W_K) K \qquad \|\Delta_K\|_\infty \le 1 \qquad (15)$$

where W_K has the same structure as in equation (12). Using results from equations (7) through (15), and rearranging the signals in Figure 7 we then obtain Figure 8. The original transport time delay problem shown in Figure 1 and 7 is now cast within the H_∞ control theory framework with multiplicative uncertainty for both the plant P and the controller K as seen in Figure 8. In this Figure 8, e_p is the plant error such that $\|e_P\|_\infty \le 1$, W_e is the performance weight or penalty on e_p, n is noise entering the system such that $\|n\|_\infty \le 1$, W_n is the penalty for noise n, d is the driver input (which can also be seen as a disturbance signal) such that $\|d\|_\infty \le 1$, and W_d is the performance weight on d. Again, the significance of the uncertainty model dW_D, for example, is that the variable transfer function d with condition $\|d\|_\infty \le 1$ captures phase uncertainty while acting as a scaling factor (since $|d| \le 1$), and $W_D(j\omega)$ captures the uncertainty profile as a function of frequency ω (since uncertainty varies and increases with ω). Once again, rework of the signals in Figure 8 yields Figure 9 where Q is an optimal controller that must be determined. The introduction of the controller Q re-casts the H_∞ nominal performance control problem (shown in Figure 7) into an H_∞ robust control problem (shown in Figure 9) [5,6]. In this case, the objective is to design an optimal control Q that minimizes the effects of the variable and uncertain transport delays modeled as $\Delta_P W_P$ and $\Delta_K W_K$.

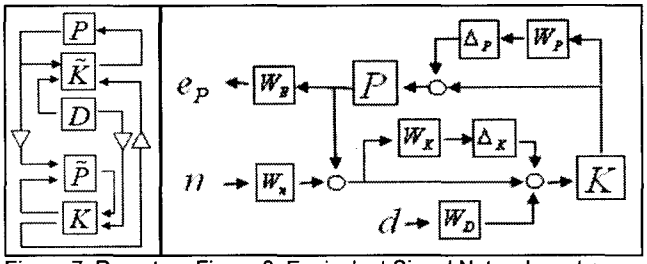

Figure 7: Remote Link Architecture

Figure 8. Equivalent Signal Network cast as an H_∞ Nominal Performance Problem.

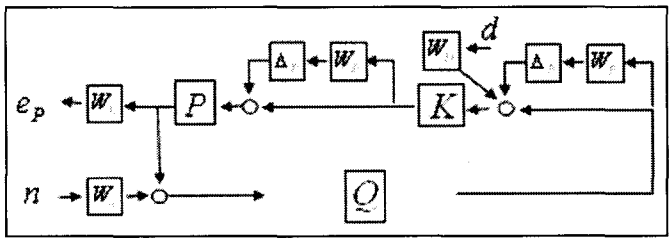

Figure 9: Remote Link Architecture cast as an H_∞ Robust Control Problem.

Figures 2, 7-9, and equations 9-15 show how to cast the original remote link *state convergence* with transport delay into an H_∞ robust control problem.

RESULTS FOR H-INFINITY CONTROL STATE CONVERGENCE

Based on the network configuration as presented in Figure 9, results are used from H_∞ robust control theory to provide a ready solution to the state and control convergence problem [7,8]. The challenging part lies in finding suitable expressions for the various performance weights as shown in Figure 9. Equally challenging is the task of capturing the prevailing dynamics of a highly non-linear system.

As a proof of concept to the problem and solution, the most relevant dynamics of a hybrid electric vehicle are captured and a system is put together as shown in Figure 2. In addition, the H_∞ robust control problem is set up as shown as in the previous section and an optimal H_∞ controller is generated. This controller is used as shown in Figure 9.

In order to test the control scheme, three simulation scenarios are run. The first scenario is shown in Figure 7, or equivalently, is shown in Figure 10 with both Q_P and Q_K set as the identity matrix. The second scenario is shown in Figure 10 but with Q_K set to the identity matrix and Q_P is set to the solution of the H_∞ robust control problem. The last scenario is shown in Figure 10 with both Q_K and Q_P set to the solution of the H_∞ robust control problem.

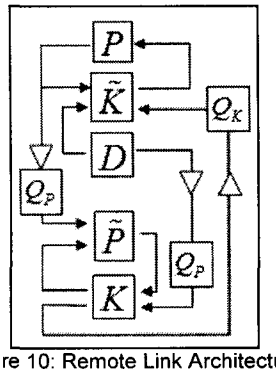

Figure 10: Remote Link Architecture
With embedded H_∞ control solution

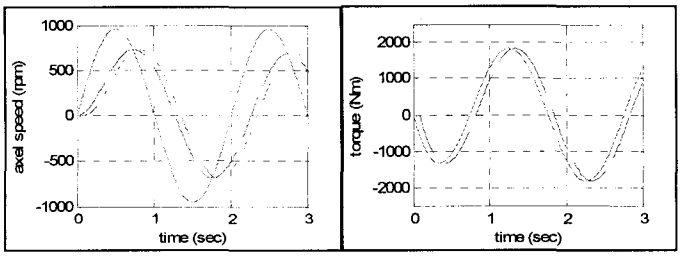

Figure 11: H_∞ control solution for scenario 1: no controller

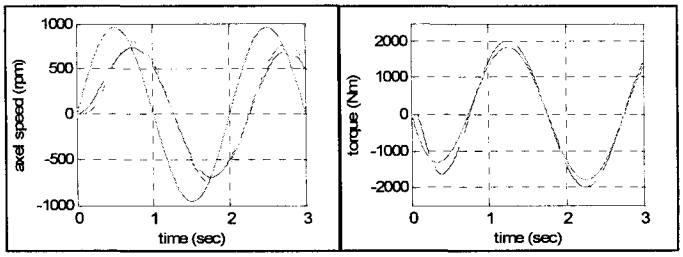

Figure 12: H_∞ control solution for scenario 2: controller for state convergence

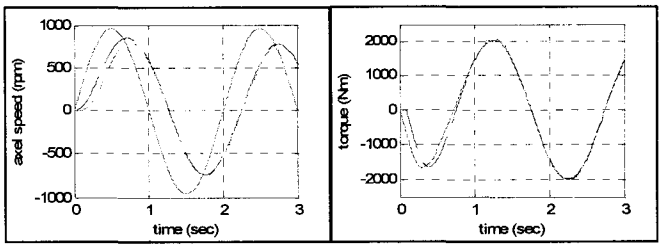

Figure 13: H_∞ control solution for scenario 3: controller for both state and actuator convergence

Figures 11-13 show the results of the simulations for the three scenarios. In all the figures above, the x-axis shows absolute time in seconds. The left most graphs show the driver command to the traction motor axial shaft speed (solid red signal) located at both the local and remote sites (see Figure 1) . The same graphs on the left also show the measured speed for both the local (dashed blue signal) and remote (dash-dot magenta signal) traction motor models. In turn, the right most graphs show the controller and inverter torque output (actuator signal) in the local (solid red) and remote (dashed blue) locations. Figure 11, corresponding to scenario 1, clearly shows the effects of the transport delay. It can be seen that with respect to absolute time, the shaft speed at the remote simulation constantly lags the speed at the local location. Figure 12 shows scenario 2 in which the *state convergence* controller at the remote location is activated. In this case the speed signals follow each other very closely, but the control signals do not. Figure 13, corresponds to case 3 when both controllers are activated (at the remote and local sites). In this case, when the system starts, an initial delay is present in both the state and control signals. However, after a few seconds, both the state and control signals converge with regard to absolute time.

ISSUES WITH IMPLEMENTATION OF THE H-INFINITY AND SLIDING MODE STATE CONVERGENCE SOLUTIONS

It has been shown that modeling transport delay as a multiplicative uncertainty and casting the *RemoteLink* within the H_∞ robust control framework promises to yield a workable solution. The framework is based on solid theoretical ground, but H_∞ robust control theory cannot handle large nonlinearities. To circumvent this problem, the H_∞ solution to the transport delay problem will utilize feedback linearization. In this case, the plant P in equation (9) could be modeled as a disturbance rejection problem with its own control design solution in which the

error arising from the feedback linearization constitutes a bounded error.

A second issue arises from the fact that some interactions of the plant dynamics emulation and the real laboratory hardware may not be well understood. The H_∞ controller is inherently conservative and will not be able to cope with non-linearity arising from both un-modeled dynamics (which can be modeled, predicted and controlled) and poorly understood emulation-hardware interactions (cannot be modeled).

In comparison, the differences between the H-infinity and sliding mode approaches are summarized as differences in inputs, assumptions, and methods for handling the time delay. The H-infinity approach utilizes standard driver inputs (throttle and steering) to effect changes in the mobility model, whereas the sliding mode approach uses fictitious skyhook accelerations (or forces) on the vehicle to effect its changes. This is a trade-off between simplicity in implementation (or plant modification) versus controllability guarantees. The H-infinity method assumes driver inputs will successfully propagate through the power system and vehicle-terrain interaction such that the desired outputs are achieved. Generally this will be a reasonable assumption. The H-infinity approach requires linear mobility and power system models while the sliding mode approach uses the nonlinear models directly. Finding a linear model of a nonlinear system is a challenge in itself, and in the process risks losing relevant dynamics. In addition, the H-infinity approach explicitly includes a time delay term in its formulation which generates closed loop control laws that explicitly compensate for those time delays. The sliding mode approach (as presented) does not explicitly take the time delay into account which limits the total closed loop system bandwidth. The states chosen for convergence are all expected to change slowly enough to be tracked within the bounds of the nominal time delay. Given these competing differences, it is not entirely clear which method is the better choice. Both are currently being pursued with the sliding mode method slated for first implementation.

CONCLUSION AND FUTURE WORK

This paper presents the *RemoteLink* effort of TARDEC's Power & Energy Initiative and the Power Budget Model for ground-based vehicles. The *RemoteLink* supports the U.S. Army's future fleet by capturing a realistic duty cycle for vehicle design and improving the Power Budget Model. Two objectives for capturing a realistic duty cycle are first, realism in the driver's experience and second, meaningful power system results. Both objectives are achieved by tightly coupling the Power and Energy SIL in real-time to the GVSL motion base. The SIL in California will receive the GVSL's live driving inputs from Michigan and provide real-time power system feedback over the internet. The *RemoteLink* effort coordinates these two driver and hardware-in-the-loop processes in order to generate a realistic duty cycle experiment. *State convergence* algorithms are a vital part of the *RemoteLink* effort, and two robust control techniques for *state convergence* are presented and yield promising results for future implementation. *State convergence* will coordinate the *powertrain observer* in the GVSL and the *vehicle dynamics observer* in the P&E SIL to create a seamless closed-loop experiment between both laboratories in Michigan and California.

The *RemoteLink* includes 4 separate efforts, including a local power system model in the GVSL (CHPSPerf), *state convergence*, an adaptive filtering algorithm, and a parameter turning algorithm. Development for *state convergence* and adaptive filtering is complete. Both improving the CHPSPerf power system model and the inclusion of a parameter turning algorithm greatly aid the *state convergence* effort. Future work involving the *RemoteLink* will address improvements to the CHPSPerf power system model including the addition of a parameter tuning algorithm.

ACKNOWLEDGEMENTS

Numerous people and organizations have contributed to the *RemoteLink* effort. The work conducted for this paper was funded, in part, by U.S. Army contract DAA-E07-02_C-L045, Combat Hybrid Propulsion System Technical Support. The authors of this paper thank the U.S. Army Research, Development, & Engineering Command (RDECOM), Tank-Automotive RD&E Center for their funding support. Additionally, the authors thank various organizations within BAE Systems, DCS, RTI and SAIC for contributions of equipment, software, models and information technology infrastructure support.

REFERENCES

1. I. Elhajj, N. Xi, W.K. Fung, Y.H. Liu, Y. Hasegawa, T. Fukuda, "Supermedia Enhanced Internet Based Telerobotics", in Proceedings of the IEEE, special issue on Networked Intelligent Robots Through the Internet, Vol. 91, No. 3, pp. 396-421, March 2003.
2. Wilford Smith and Kurt Wehmueller, "Detailed Simulation and Development of Hybrid Power Systems Energy Management Architectures", Paper presented at the 4th International AECV Conference, January 2002.
3. Ronnie Wright, Jarrett Goodell, Wilford Smith, and Patrick Nunez, "A Delay Compensation Strategy For Improved Remote Link Control Over A Long Haul Communications Channel", Paper presented at the 6th International AECV Conference, June 2005.
4. Wilford Smith and Patrick Nunez, "Power and Energy Computational Models for the Design and Simulation of Hybrid-Electric Combat Vehicles", SPIE Paper No. 5805-02, Paper Presented at Simulation Science IX, Orlando, FL, 28 March – 1 April 2005.
5. Marc Compere, Miguel Simon, John Kajs, and Mike Pozolo, "Tracked Vehicle Mobility Load Emulation for a Combat Hybrid Electric Power System", Paper

presented at the 6th International AECV Conference, June 2005.
6. Jean-Jacques Slotine and Weiping Li, *Applied Nonlinear Control*, Prentice Hall, 1991.
7. J. Doyle, B. Francis, and A. Tannenbaum; *Feedback Control Theory*, MacMillan, 1990.
8. K. Zhou, J. Doyle, and K. Glover; *Robust and Optimal Control,* Prentice-Hall, 1996.

CONTACT

Mr. Goodell may be contacted at Science Applications International Corporation, 8303 N. Mopac Expwy, Suite B-450, Austin, Texas 78759, jarrett.d.goodell@saic.com.